ELSEVIER

The J- and H-bands of organic dye aggregates

A. Eisfeld *, J.S. Briggs

Theoretische Quantendynamik, Universität Freiburg, Hermann-Herder-Strasse 3, D-79104 Freiburg, Germany

Abstract

Certain molecular aggregates consisting of organic dyes are remarkable in exhibiting an intense and very narrow absorption peak, known as a J-band, which is red-shifted away from the region of monomer absorption. Apart from those dyes showing the J-band on aggregation, there are also dyes where the absorption maximum is shifted to higher energies. The width of the resulting absorption band (called an H-band) is comparable to that of the monomeric dyes and shows a complicated vibrational structure. Following our analysis of the J-band spectra of polymer aggregates using the CES approximation [A. Eisfeld, J.S. Briggs, Chem. Phys. 281 (2002) 61], a theory that includes vibrations explicitly, we show that the same approximation can account for measured H-band spectra. Using simple analytical forms of the monomer spectrum the origin of the widely different shapes of H- and J-bands is explained within the CES approximation.
© 2005 Elsevier B.V. All rights reserved.

Keywords: J-aggregates; H-band; Organic dyes; Absorption lineshape; Vibrations; Excitons

1. Introduction

Since the discovery of the J-band or Scheibe-Peak (Jelley, Scheibe) [1–3] of the pseudoisocyanine (PIC) molecular aggregate, an enormous amount of work has appeared concerning the light absorption properties of such organic dyes [4–10], and in recent years many new applications have been discussed [11–14]. In the 30s of the last century Scheibe made comprehensive studies using different dyes, solvents, concentrations and temperatures, concluding in 1937 that the change of the absorption spectrum is due to "reversible polymerisation", i.e. aggregation of the dye monomers into loosely bound polymers [3]. One year later this picture was supported by Franck and Teller [15] who used the exciton theory of Frenkel [16].

During his studies, Scheibe found that, for some dyes, the aggregate absorption band is red-shifted with respect to that of the monomer. These are the J-aggregates showing a very narrow band whose position is well-predicted by a theory ignoring intramolecular vibrations. By con-

trast, other dyes showed a shift towards the blue (i.e. higher absorption energies) and were termed H-aggregates (hypsochromic shift). Unlike the J-band, the lineshape of the H-band generally shows a rich vibrational structure and has a width of the order of that of the monomer band. Some substances, indeed PIC itself, exhibit both a J-band and a H-band on aggregation. As a result of this complicated vibrational structure, although there exists a considerable literature on the simpler case of the J-band, there have been only a few theoretical articles which address the lineshape of H-aggregates, e.g. Refs. [17–20].

A common treatment in the calculation of excitonic absorption spectra is to start from a purely electronic theory but to treat the energy-levels of each monomer as random variables described by, e.g., a Gaussian distribution. To obtain the absorption spectrum the Hamiltonian of an aggregate consisting of say 500 monomers is diagonalised for a large number (typically several thousand) of cases and the stick spectra obtained for each aggregate are summed over. This quite successful approach is used, e.g., in Refs. [8,21] to describe aggregate spectra. However, the assumption of a single Gaussian does not account for a vibrational progression in either monomer or aggregate. In

---

* Corresponding author.
E-mail address: alexander.eisfeld@physik.uni-freiburg.de (A. Eisfeld).

contrast the CES theory, which is used in this work, is primarily concerned with the treatment of internal vibrations. These have a strong influence on the lineshape of the monomeric dyes, which usually show a pronounced vibrational progression. The averaging performed in the statistical theories, which mimics the influence of the environment or low-frequency modes of the monomer itself, is described in the CES approximation by assigning a lineshape to each peak of the monomer progression in order to fit the known monomer absorption lineshape. It should also be stressed, that a purely electronic theory with disorder is not able to reproduce the vibrational structure of the H-band.

The full diagonalisation of the aggregate Hamiltonian when not only electronic but also vibrational degrees of freedom are included is hardly tractable for long aggregates. Precisely to avoid this problem, in previous studies [22–24] we used the CES-approximation. This method is extremely simple and uses as input the (measured) lineshape of the monomer, in order to calculate the lineshape of the aggregate. In particular in Ref. [22], which we will refer to as **I**, it was shown that the CES-approximation gives very good agreement with measured J-aggregate spectra and also, via the transition dipole properties of the monomers, the theory is able to give information on the possible geometry of the aggregates.

In our previous work on J-aggregates, the coupling strength between the monomers, which we call C, was large compared to the width, called Δ of the monomer absorption. In the nomenclature of Simpson and Peterson [25], $C/\Delta \gg 1$ is called the strong coupling regime. In the cases considered, this also implies that, since the shift is to lower energies of absorption, the J-band appears at an energy below the $0 \rightarrow 0$ lowest vibronic transition of the monomer. As was shown in [24] in this situation the CES approximation predicts a single narrow line, shifted by an energy C from the mean of the monomer absorption. However, when the shift is to higher energies, as in H-aggregates, the aggregate absorbs in a region where the monomer itself may absorb. In this case, depending on the magnitude of C, the CES approximation predicts several peaks in the aggregate spectrum. Hence, as shown below in detail, the qualitative differences in the H-aggregate and J-aggregate spectra are explained by the CES approximation. The aim of this paper is to show that the approximation gives also good quantitative agreement with the shape of H-aggregate spectra in the difficult case of intermediate coupling $C/\Delta \approx 1$. In addition, an analysis of the CES approximation applied to the simple case of stick spectra, where the results can be obtained analytically, will show the precise origin of the widely different shapes of J- and H-bands.

Specifically we will compare the CES-approximation with experiment in the case of H-aggregate spectra of PIC and of pinacyanol (1,1′-diethyl-2,2′-monocarbocyanine), which was studied long ago by Scheibe [26] but whose spectral shapes have never been explained. We will also use more recent data by Al-khouri [27]. We will show that in the case of pinacyanol, assuming a simple aggregate geom-etry (a one-, two- or three-dimensional array with parallel monomer transition dipoles), the CES approximation gives very good agreement with the different lineshapes of the H-band for a variety of concentrations. The calculations require as parameter only the coupling strength C and this parameter alone decides the shape of the complete H-band. However it is also necessary to allow for an overall shift S of the complete absorption band occurring on aggregation.

2. The CES-approximation

The absorption cross-section for light of frequency ω polarised in direction $\hat{x}$ is given by

$$\sigma_{\hat{x}} = \frac{4\pi}{c} \omega \, \text{Im}(\hat{x} \cdot \boldsymbol{\alpha} \cdot \hat{x}) \tag{1}$$

where $\boldsymbol{\alpha}(\omega)$ is the frequency-dependent ground-state polarisability tensor. For the non-interacting monomers with total (electronic plus vibrational) Hamiltonian H_0, one has

$$\boldsymbol{\alpha}^{\text{M}}(\omega) = -\sum_n \boldsymbol{\mu}_n \langle g_n(E_0 + \hbar\omega) \rangle \boldsymbol{\mu}_n \tag{2}$$

where the monomer Green operator $g(E) = (E - H_0 + \mathrm{i}\delta)^{-1}$ and $g_n = \langle \pi_n | g | \pi_n \rangle$. The state $|\pi_n\rangle$ denotes the electronic state in which monomer n is excited and all other monomers are in their ground electronic state. The energy E_0 is the total ground state energy of non-interacting monomers and the brackets $\langle \cdots \rangle$ in (3) denote an expectation value over the ground vibrational state of the monomers. The $\boldsymbol{\mu}_n$ are the transition dipoles located at each monomer site. For the interacting monomers the corresponding expression for the aggregate polarisability is,

$$\boldsymbol{\alpha}^{\text{A}}(\omega) = -\sum_{nm} \boldsymbol{\mu}_n \langle G_{nm}(E_0 + \hbar\omega) \rangle \boldsymbol{\mu}_m \tag{3}$$

Where $G(E) = (E - H_0 - V + \mathrm{i}\delta)^{-1}$ is the aggregate Green operator involving the total dipole–dipole interaction operator V.

If we assume, as the simplest case, that in the aggregated state, all transition dipoles have identical orientation, then only one band appears in the spectrum for an arbitrary linear polarisation. The derivation of the CES approximation is given in Refs. [23,24] and in this case the aggregate absorption cross-section becomes (for N identical monomers $\langle g_n \rangle \equiv g(\omega)$ is independent of n and putting $|\boldsymbol{\mu}_n| = \mu$),

$$\sigma^{\text{A}}(\omega) = \frac{4\pi}{c} \omega \, N\mu^2 \, \text{Im} \left(\frac{g(\omega)}{1 - Cg(\omega)} \right), \tag{4}$$

where the monomer absorption cross-section is

$$\sigma^{\text{M}}(\omega) = \frac{4\pi}{c} \, N\mu^2 \, \text{Im} \, g(\omega). \tag{5}$$

The interaction strength C is simply given by

$$C = \sum_n V_{nm}, \tag{6}$$

where n denotes the indices specifying the position of monomer n in a periodic one, two or three-dimensional lattice with one monomer per unit cell.

The real and imaginary parts of $\boldsymbol{\alpha}^M$ and $\boldsymbol{\alpha}^A$ are not independent but are connected by a Kramers–Kronig dispersion relation. Since the $\boldsymbol{\mu}_n$ are independent of energy this relation connects the real and imaginary parts of $g(\omega)$ and this function describes the shape of the monomer absorption band. Putting $E = E_0 + \hbar\omega$, the energy-dependent part of the polymer absorption spectrum is obtained from Eq. (4) as,

$$\sigma^A \propto G_I(E) \equiv \text{ Im } G(E) = \text{ Im } \frac{g(E)}{1 - Cg(E)}. \tag{7}$$

To begin, and for purposes of later orientation, let us ignore vibrations altogether and consider that the monomer absorption consists of a single line, whose energy we take as the zero of energy. The monomer function $g(E)$ is given by

$$g(E) = \lim_{\delta \to 0} \frac{1}{E + i\delta} \tag{8}$$

and $\text{Im } g(E) = -i\pi\delta(E)$ gives the absorption profile. Then, from Eq. (7),

$$G(E) = \lim_{\delta \to 0} \frac{1}{(E - C) + i\delta} \tag{9}$$

and $\text{Im } G(E) = -i\pi\delta(E - C)$. Thus, in this trivially simple case, the CES approximation gives the exact result of exciton theory; the polymer absorption is also a single line shifted by the coupling C. Also for later comparison we show in Fig. 1 the function $g_R^{-1}(E)$ where g_R is the real part of $g(E)$. Polymer absorption occurs at the pole $g_R^{-1} = C$ (since $g_I = 0$ at the pole, where g_I is the imaginary part of $g(E)$). In this simple case $g_R^{-1} = E$ and the pole occurs at $E = C$ shown in Fig. 1 for $C/E = \pm 2$.

Now we turn to the non-trivial case where vibrations are included. For the case of a single vibrational progression, as appears to be a good approximation for the dye monomers considered here, in the absence of coupling to other monomer or solution vibrational modes, the monomer absorption band is described by,

$$\text{Im } g(E) = -\pi \sum_{j=0} |f_j|^2 \delta(E - \epsilon_j), \tag{10}$$

where $|f_j|^2$ are Franck–Condon (FC) factors for a transition from the vibrational ground-state of the ground electronic state to the vibrational level j, with energy ϵ_j, of the upper

electronic state. Now we take ϵ_0 as the zero of energy and the vibrational spacing as the unit of energy. From the dispersion relation, this "stick" spectrum is given by the function

$$g(E) = \lim_{\delta \to 0} \sum_{j=0} \frac{|f_j|^2}{E - \epsilon_j + i\delta}. \tag{11}$$

For simplicity of illustration we take the ground and excited state Born–Oppenheimer potential curves to be the same harmonic curve but with a shift d in their respective minima. Then, if the ground vibrational state amplitude is a, the FC factors follow a Poissonian distribution

$$|f_j|^2 = \frac{x^j}{j!} e^{-j} \tag{12}$$

in the dimensionless variable $x = (d/a)^2$. The resulting monomer stick spectrum is shown in Fig. 2(a) for the case $x = 1$ so that the mean energy of the monomer spectrum is at $+1$. The polymer spectra for different coupling strength C are shown in Fig. 2 also. Note that the exact sum rules on spectral moments are satisfied in the CES approximation [23]. In particular the total absorption strength $\sum_{j=0} |f_j|^2$ is conserved and the first moment of the polymer absorption band is shifted by an energy C with respect to that of the monomer.

For negative values of C, the polymer spectra are redshifted with the strongest line appearing in the energy region below the onset of monomer absorption. As $|C|$ becomes larger this line carries more and more of the oscillator strength as the polymer absorption in the region of monomer absorption diminishes rapidly (see Fig. 2(b)–(d)). This single peak forms the J-band in this case and corresponds, in an exciton picture with no vibrations, to absorption into the $k = 0$ exciton state. Here we have included vibrations but still the polymer absorption narrows into a single line, carrying the whole of the oscillator strength as $|C| \to \infty$, the case of strong coupling.

For positive values of C (blue-shift) the situation is completely different, as shown in Fig. 2(e)–(g). For the same values of $|C|$ as for the J-band, the polymer spectrum stays relatively broad as the coupling strength increases and even for the "strong coupling" case $C = +3$ the absorption is distributed over several vibronic lines. This is the case of the H-band where experiment shows generally several peaks comprising a relatively broad absorption spectrum, in qualitative agreement with the spectra of Fig. 2. To summarise, the CES approximation predicts a narrow J-band for monomer–monomer interactions leading to a red shifted polymer spectrum and a relatively broader H-band for blue-shifted polymer spectra, both corresponding to the experimental situation. Note that the width of the monomer spectrum in Fig. 2(a) is given by $\Delta = 1$, in units of the harmonic oscillator eigenvalue spacing, so that Fig. 2(b) and (e) correspond to weak coupling, Fig. 2(c) and (f) to intermediate coupling and Fig. 2(d) and (g) to strong coupling, in the sense of Simpson and Peterson [25].
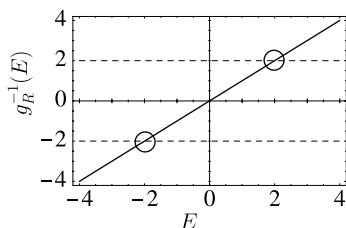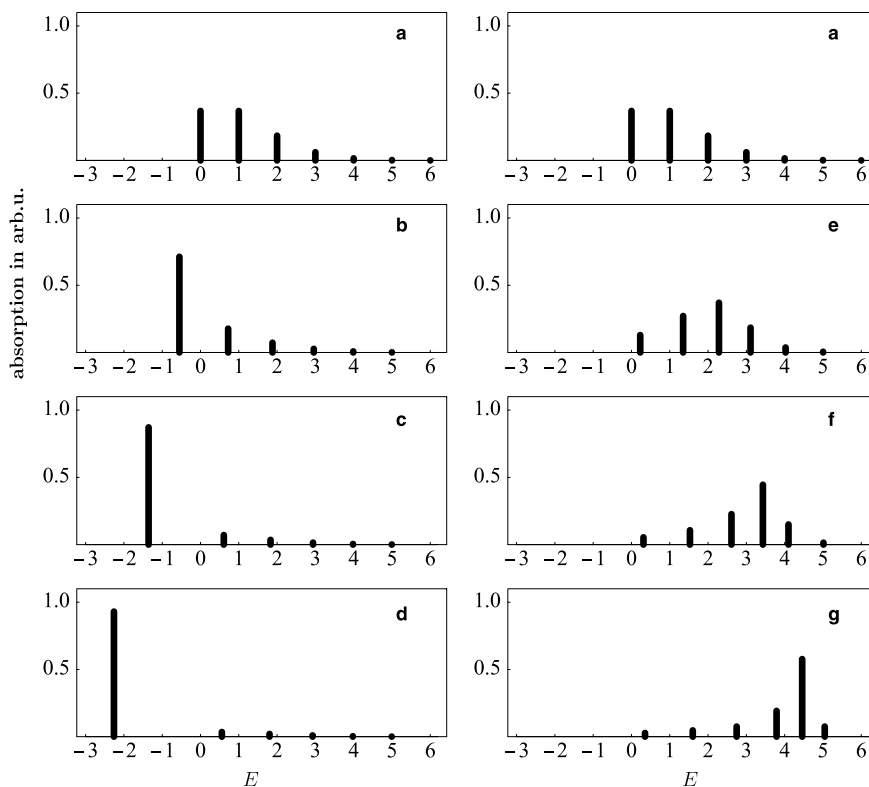

Fig. 1. The monomer function $g_R^{-1}(E)$ in the case of a single absorption line at $E = 0$. The poles of the aggregate function $G(E)$ are marked by circles.

Fig. 2. (a) Monomer absorption spectrum for $x = 1$. The polymer absorption spectra in CES approximation for C values of: (b) -1; (c) -2; (d) -3; and (e) $+1$; (f) $+2$; (g) $+3$.

The physical origin of the difference in polymer spectra, according to whether the shift is out of or into the energy regions where the monomer absorbs, can be established by considering the analytic form of the energy-dependent part of the polymer absorption function $G_I(E)$ in Eq. (7). Since C is real and the imaginary part of g is zero except at $E = \epsilon_j$ (see Eq. (10)), then the polymer absorbs at the poles $E = E_i$, and at these poles $g_I(E_i) = 0$ so that one may expand

$$g_R(E) = g_R(E_i) + (E - E_i)\frac{\partial}{\partial E}g_R(E)\Big|_{E_i} \qquad (13)$$

and substitution in Eq. (7) leads to the simple result that the absorption strength at each pole is proportional to $\left[\frac{\partial}{\partial E}g_R^{-1}(E)\big|_{E_i}\right]^{-1}$, i.e. to the inverse of the slope of the curve of $g_R^{-1}(E)$ at the pole. This curve is shown in Fig. 3, calculated from the monomer spectrum of Fig. 2. This is to be contrasted with the vibrationless case shown in Fig. 1. In that case the polymer absorption band, for C negative or positive is a single peak located at the intersection of the sloping line $g_R^{-1}(E) = E$ and the horizontal lines $g_R^{-1}(E) = C$. The slope at the poles is constant, equal to unity, i.e. absorption strength is conserved. By contrast, in Fig. 2 the curve $g_R^{-1}(E)$ is zero at the energies of monomer absorption, i.e. at each vibronic level shown in Fig. 2(a). For large $|E|$ the curve is asymptotic to the line $g_R^{-1} = E - 1$, since the mean energy of the monomer spectrum is now at $E = 1$, as in the vibrationless case of Fig. 1. However, since the monomer does not absorb below
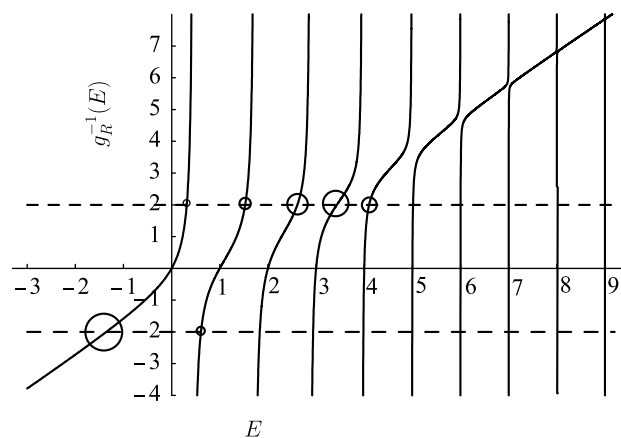

Fig. 3. The monomer function $g_R^{-1}(E)$ for the absorption spectrum of Fig. 2(a). The circles denote the poles of the polymer function carrying significant oscillator strength for $C = -2$ (J-band) and $C = +2$ (H-band).

$E = 0$, this asymptote is arrived at much more rapidly for negative E than for positive E. This is the key to the difference between J- and H-bands.

The polymer poles occur where $g_R^{-1}(E) = C$, i.e. at the intersections of the curve g_R^{-1} with the horizontal line denoting a fixed value of C. These poles are shown in Fig. 3 for the strong coupling case $C = \pm 2$. For $C = -2$, the red-shifted case, the slope at the intersections within the monomer band is large near to the infinities, giving very low absorption strength at these poles. By contrast, the single pole at negative energies has a slope approaching unity

(from above). Hence this pole carries virtually all the oscillator strength. It is the J-band absorption and is an example of a co-operative effect familiar in other branches of many-body physics, e.g., the plasmon or the nuclear giant dipole resonance. In strong coupling a single co-operative level splits off from the one-body absorption spectrum and carries with it virtually all the oscillator strength of the N-body aggregate.

Considering now the blue-shifted case of $C = +2$ one sees immediately the origin of the different behaviour. Since the monomer absorbs in the positive energy spectral region, at the polymer poles, shown in Fig. 3 for $C = +2$, the slope is not close to infinity and the absorption is spread over a number of poles. This is the H-band. Only at C values $\gtrsim +5$ is the vibrationless asymptote essentially achieved and a situation equivalent to the J-band realised.

The physical interpretation of J- and H-band characteristics is also clear. The J-band is shifted to energies where monomer electronic vibrational coupling is absent. Absorption is into a single state with negligible vibrational broadening corresponding to rapid transfer of electronic excitation along the polymer in the co-operative excitonic state; so rapid that vibrational relaxation cannot occur before the exciton transfers to the next monomer. Hence this situation corresponds to the vibrationless case. By contrast the H-band is shifted into a region where monomer vibronic coupling is still operative. Absorption is into several vibronic states and only for extreme strong coupling C is absorption concentrated into a single line and a situation similar to the J-band is reached.

From the above results one sees that the Simpson–Peterson criterion is incomplete. Quite how strong the coupling must be to achieve the J-band-like "strong" coupling behaviour depends upon the sign of the spectral shift and in particular on the monomer absorption in the wings of the spectrum. Strong coupling behaviour with a narrow, almost vibrationless absorption is only achieved when the polymer absorbs at energies where the monomer absorption is vanishingly small. This point is illustrated very clearly analytically in an extreme case of a single, Lorentz broadened monomer absorption line, i.e.

$$g(E) = \frac{1}{E + i\Gamma/2} = \frac{E - i\Gamma/2}{E^2 + \Gamma^2/4}. \tag{14}$$

Then, from Eq. (7)

$$\mathrm{Im}\, G(E) = \mathrm{Im}\, \frac{1}{E - C + i\Gamma/2} = \frac{-\Gamma/2}{(E - C)^2 + \Gamma^2/4}. \tag{15}$$

Hence the polymer absorption is a shifted Lorentz profile of exactly the same width; there is no narrowing of the spectrum however large the coupling and whatever the sign, since the monomer absorption drops off only quadratically with energy for both positive and negative energy.

3. Comparison with experiment

The strategy to implement the CES-approximation in the case of experimental data is to extract the monomer bandshape function $g_I(\omega)$ from the *measured* monomer absorption cross-section according to Eq. (5). Such monomer spectra correspond often to a single vibrational progression as in Fig. 2 but where each individual line is broadened by coupling to other modes of the monomer or to solvent modes, etc. Nevertheless, in the case of a continuous monomer spectrum, using the Kramers–Kronig dispersion relation the corresponding $g_R(E)$ can also be calculated. This complex function $g(E)$ is then substituted in the function $G(E)$, whose imaginary part gives the aggregate lineshape function according to Eq. (7). The value of

Table 1
The parameters used in Fig. 5

c_d molar	F	C (cm^{-1})	S (cm^{-1})	Fig.
4.44×10^{-6}	3.17	0	0	5(a)
1.33×10^{-5}	3.22	580	200	5(f)
4.44×10^{-5}	3.85	1010	400	5(g)
1.33×10^{-4}	3.42	1370	480	5(h)
4.44×10^{-4}	3.86	1690	700	5(i)

Table 2
The parameters used in Fig. 6

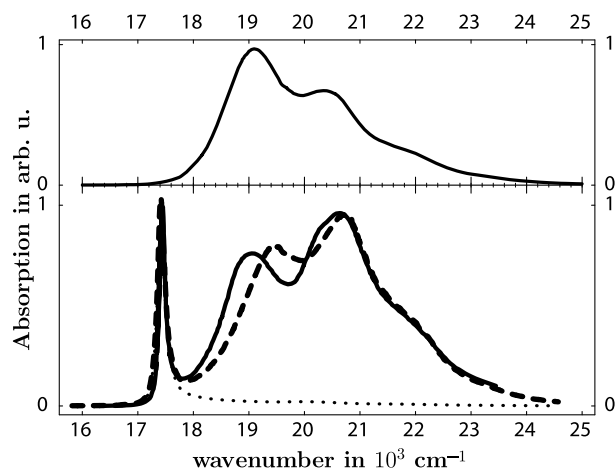| c_d molar	F	C (cm^{-1})	S (cm^{-1})	Fig.
2.3×10^{-6}	3.13	0	0	6(a)
2.9×10^{-5}	3.62	580	100	6(h)
1.6×10^{-4}	3.53	1260	460	6(i)
3.5×10^{-4}	3.55	1410	500	6(j)
5.7×10^{-4}	3.59	1550	550	6(k)
1.1×10^{-3}	3.46	1760	610	6(l)
2.0×10^{-3}	3.52	1910	630	6(m)

Fig. 4. *Top:* The measured monomer spectrum at a concentration of 1×10^{-5} mol/L at $T = 20\,^{\circ}$C in methanol. *Bottom:* continuous line is the measured aggregate spectrum at 2.25×10^{-3} mol/L in 0.01 M NaCl solution. The dotted line is the theoretical J-band spectrum, the dashed line is the sum of theoretical J- and H-band contributions.

the real energy parameter C is then adjusted to obtain the best fit of the shape of the measured aggregate spectrum. These fits have been made simply by trial and error to obtain the best overall agreement with the most prominent features in the aggregate spectrum. Generally the sensitivity of the spectral shape is such that C can be varied by approximately ± 30 cm^{-1} before there are appreciable changes, so that this can be viewed as the uncertainty in the C values given in Tables 1 and 2.

Following an early demonstration that the CES approximation can explain qualitatively the J-band shape in polymer pseudoisocyanine chloride (PIC) [28], in paper **I** we showed that an excellent reproduction of J-band shapes and positions is obtained for a variety of dyes (PIC, TDBC

and derivatives). In the case of PIC, as shown in Fig. 4 (solid line), the aggregate spectrum shows not only the J-band, reproduced in **I** with a value of $C = -1900$ cm^{-1}, but also prominent absorption in the region of monomer absorption, although the band shape is very different and the centre is blue-shifted from that of the monomer. If we assign the absorption to a blue-shifted H-band with $C = +500$ cm^{-1}, using the same measured monomer spectrum as input for both J- and H-band contributions, we obtain the total spectrum shown in Fig. 4 (dashed line). The agreement is very good in the region of the J-band and on the high energy side of the the H-band. There is some discrepancy around 19,000 cm^{-1} which may indicate a breakdown of the CES approximation. However, one notes that this is
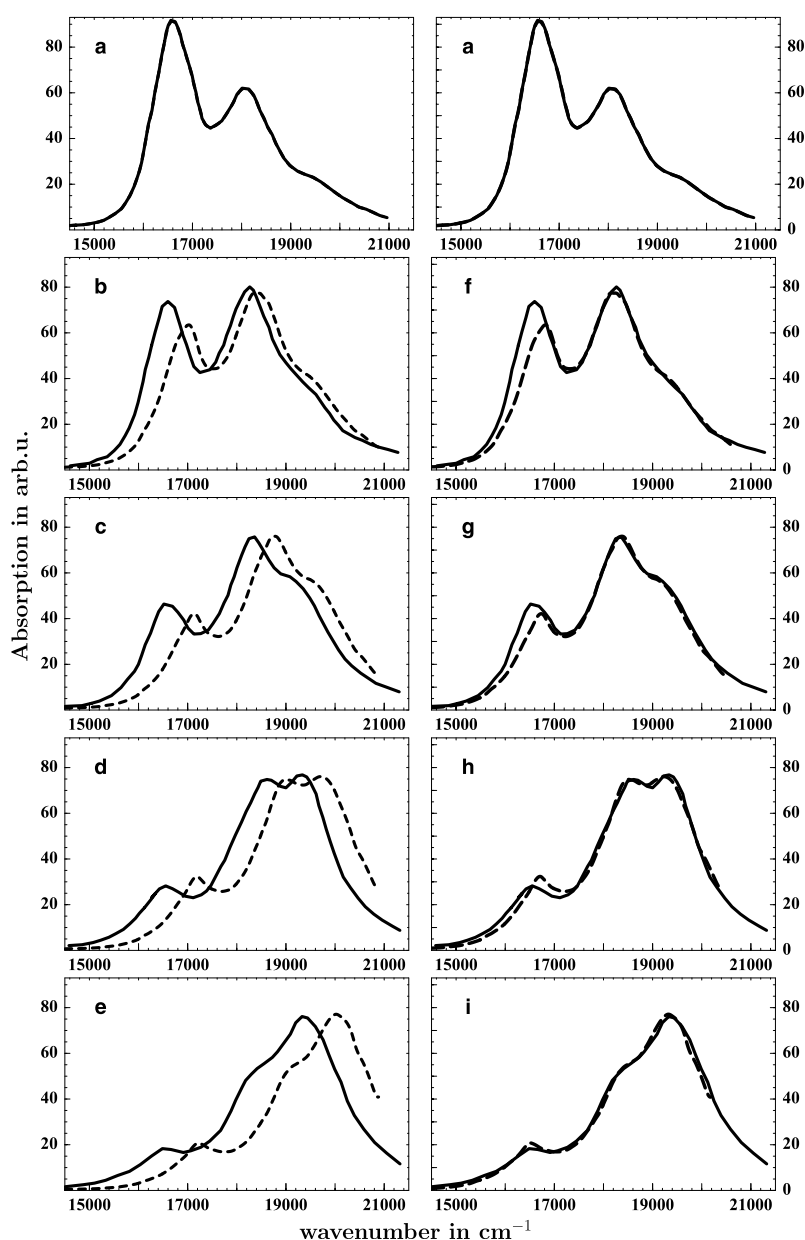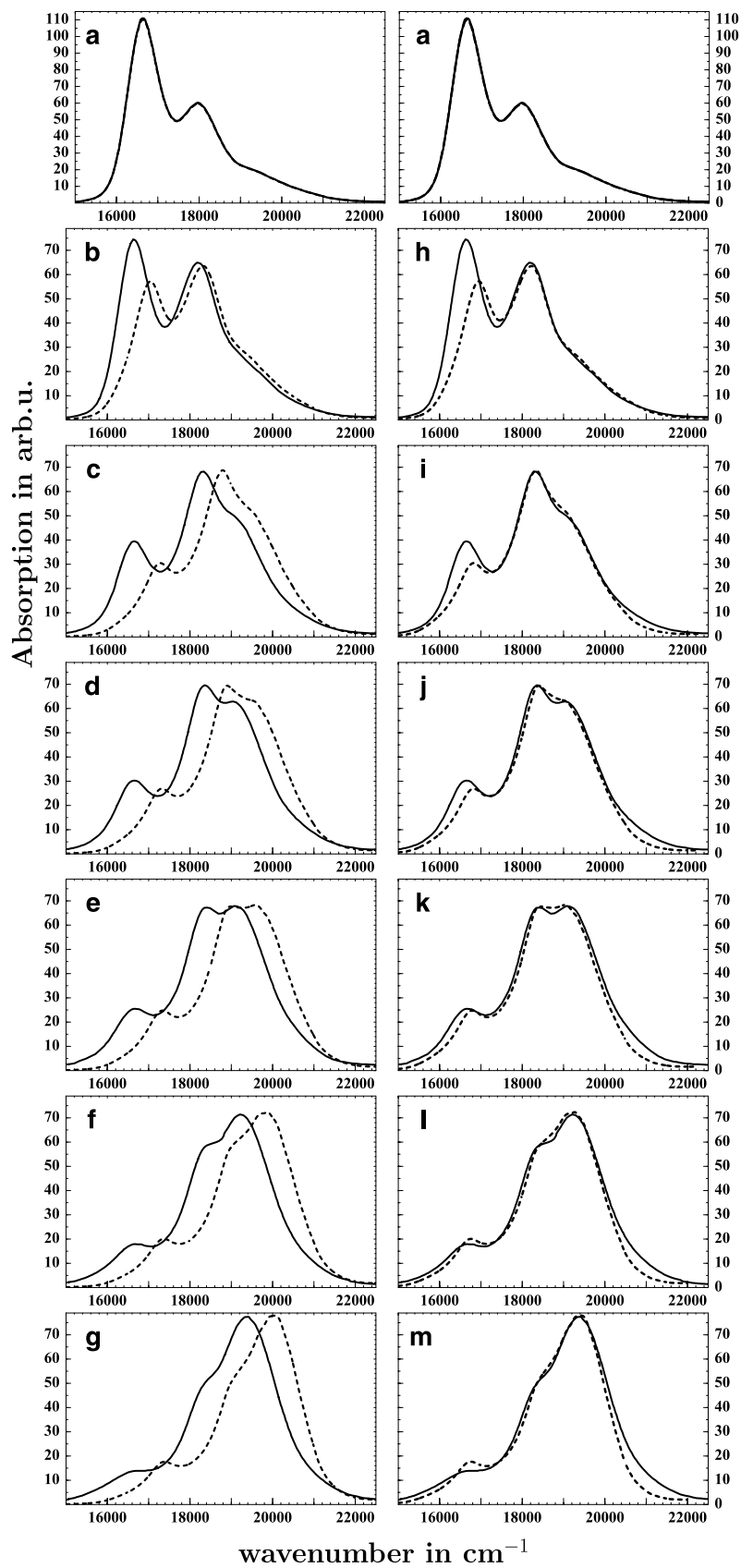

Fig. 5. Spectra of pinacyanol from Ref. [26]. Full curves experiment, dashed curves CES approximation. (a) Monomer spectrum. The figures from top to bottom are aggregate spectra for increasing concentration. In the right-hand figures (f)–(i) the theoretical curves have been shifted by an energy S (see Table 1).

Fig. 6. Spectra of pinacyanol from Ref. [27]. Full curves experiment, dashed curves CES approximation. (a) Monomer spectrum. The figures from top to bottom are aggregate spectra for increasing concentration. In the right-hand figures (h)–(m) the theoretical curves have been shifted by an energy S (see Table 2).

precisely where the monomer spectrum has its dominant peak, so that the discrepancy may be due to residual monomer contamination. Nevertheless, all major features of the measured PIC aggregate spectrum [29] are reproduced.

Next we turn to the case of pinacyanol. The measured spectra (almost 70 years old) of Scheibe [26] are shown as solid lines in Fig. 5 (in aqueous solution at 20 °C) and those of Al-khouri [27] in Fig. 6 (in aqueous solution with 7.5 % v/v ethanol at room temperature). One notes a systematic blue shift of the mean energy as the dye concentration increases and a corresponding change in the shape of the H-aggregate spectra. We take the spectra at the lowest concentration (Fig. 5(a)) for Scheibe and Fig. 6(a) for Al-Khouri, respectively) to represent the monomer spectrum. Our calculated spectra using a C value to best reproduce the *shape* of the experimental spectra are shown in Figs. 5(b)–(e) and 6(b)–(g). To obtain the correct height of the spectra we have also adjusted slightly the absolute values of the calculated spectra. From the exact sum rule, the area under each curve should be the same in a one-band theory so that the relevant scaling parameter is $F = $ (peak height/ peak area) and these factors are shown in Table 1 (Scheibe data) and Table 2 (Al-Khouri data).

From the comparison on the left-hand figures in Figs. 5 and 6, one notes a good agreement in shape but a discrepancy in absolute position. Therefore each calculated spectrum, without change of shape, has been moved to lower energies by a shift S. The results are shown in the right-hand figures (Figs. 5(f)–(i) and 6(h)–(m)). The agreement is now good in all cases. For example, in the Scheibe data, the emergence of the peak near to 19,500 cm^{-1} is accurately reproduced as concentration is increased. Even fine details such as the small dip at 19,000 cm^{-1} on Fig. 5(h) are reproduced. The parameters C, S and F for the two sets of data are given in Table 1 (Scheibe) and Table 2 (Al-Khouri). Solely for the weak-coupling cases Fig. 5(f) and (g), 6(h) and (i), is there a discrepancy in the spectral region around 16,500 cm^{-1}. However, as in the case of PIC, this discrepancy occurs precisely where the monomer has its maximum absorption and may possibly be due to residual monomers at low concentration.

The analysis of the two fitting parameters C and S as a function of dye concentration provides evidence, even if only circumstantial, that the effective state of aggregation changes with concentration. Both the coupling strength C and the shift S as function of the dye concentration $c_{\rm d}$ can be fitted by a linear function of the logarithm of $c_{\rm d}$. For the Scheibe data we find

$$S(c_{\rm d}) = 340~{\rm cm}^{-1}\log(c_{\rm Dye}) + 1800~{\rm cm}^{-1} \quad (16)$$
$$C(c_{\rm d}) = 700~{\rm cm}^{-1}\log(c_{\rm Dye}) + 4000~{\rm cm}^{-1}. \quad (17)$$

Similarly for the Al-Khouri data one has

$$S(c_{\rm d}) = 166~{\rm cm}^{-1}\log(c_{\rm Dye}) + 1088~{\rm cm}^{-1} \quad (18)$$
$$C(c_{\rm d}) = 712~{\rm cm}^{-1}\log(c_{\rm Dye}) + 3877~{\rm cm}^{-1}. \quad (19)$$

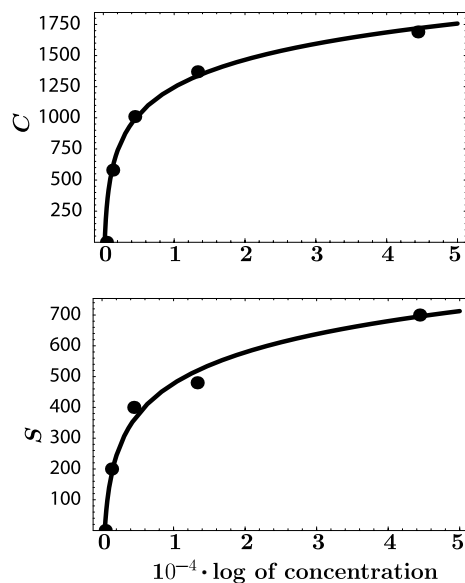These curves are plotted in Figs. 7 and 8.

Fig. 7. *Top:* calculated couplings C as function of the dye concentration. *Bottom:* calculated shifts S as function of the dye concentration. The lines are fitted curves from Eqs. (17) and (16).
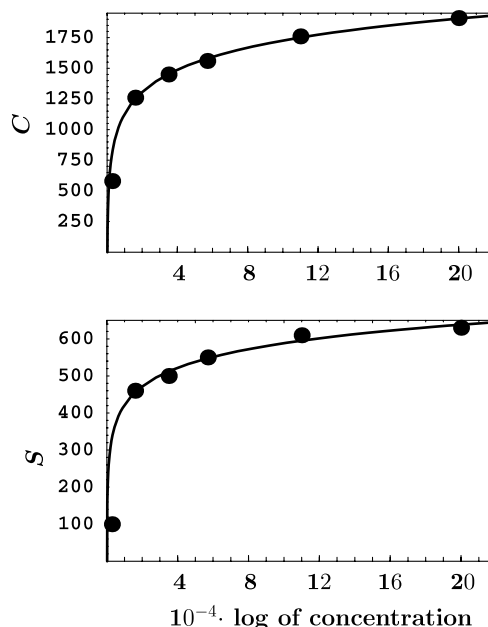

Fig. 8. Same as Fig. 7. The lines are fitted curves from Eqs. (19) and (18).

One notes the broad similarity between the behaviour of C and S in both cases and the apparent tendency to saturate with increasing concentration, as one might expect. The coupling C (Eqs. (19) and (17)) appears relatively insensitive to solvent character which would support the view that the state of aggregation or the geometry of the aggregate conformation changes in the same way with concentration in the two sets of experiments. The shift S appears to depend upon the solvent. This could indicate a solvent-dependent depression of ground-state energy

which changes as the dye conformation changes with concentration, or it could be linked to the changes in C itself, i.e. how quickly the sum in Eq. (6) converges with increasing aggregate size. Suffice it to say that, within the CES approximation, the changes in C and S with concentration appear to be correlated and this could throw light on the conformation of the H-aggregate.

4. Conclusion

In summary we have shown that the CES theory, known to be well suited to describe absorption spectra of J-aggregates, is also able to describe H-aggregate spectra, even in the regime of weak and intermediate coupling. However, unlike the case of J-aggregates, where the J-band appears at a certain concentration and then does not change shape or position appreciably, the H-aggregates exhibit a strong dependence on shape (through C) and position (through S) as the concentration changes.

There can be several reasons for a change in C. Within our model of monomers interacting through dipole dipole forces, one has

$$V_{nm} = \frac{\mu^2}{r_{nm}^3}(1 - 3\cos(\alpha)), \qquad (20)$$

where r_{nm} is the distance separating monomer n and m, and α is the angle between the transition dipole moment and an axis of the aggregate. Hence there is the possibility that, for the H-aggregate either the angle α, the separation r_{nm}, or both, change with concentration. Alternatively, although the r^{-3} dependence implies that the sum in Eq. (6) converges for states of high aggregation, for low concentrations the aggregate may be dominated by low-N species (dimers, trimers) for which C can change considerably. Indeed that C *increases* with concentration supports this contention.

Apart from the observation of the correlation with changes in C, the changes in the shift S are harder to explain in the present state of experimental knowledge of the conformation of H-aggregates. From this point of view it would be interesting to see how S and C change in different solvents, as a function of temperature, or perhaps as function of pressure as was done for TDBC/C8O3 in Refs. [30,31].

Clearly, the theory needs to be developed further to enable C and S to be obtained from first principles rather than to be inserted as fit parameters. Then the theory could help to understand the geometrical arrangement of more complicated aggregates, e.g., amphiPIPES [32].

Acknowledgement

References

[1] E.E. Jelley, Nature 138 (1936) 1009.
[2] G. Scheibe, Angew. Chem. 49 (1936) 563.
[3] G. Scheibe, Angew. Chem. 50 (1937) 212.
[4] R.L. Fulton, M. Gouterman, J. Chem. Phys. 35 (1961) 1059.
[5] M. Kasha, Radiat. Res. 20 (1963) 55.
[6] H. Sumi, J. Phys. Soc. Jpn. 32 (1972) 616.
[7] E.W. Knapp, Chem. Phys. 85 (1984) 73.
[8] H. Fidder, J. Knoester, D. Wiersma, J. Chem. Phys. 95 (1991) 7880.
[9] C. Warns, P. Reineker, I. Barvík, Chem. Phys. 290 (2003) 1.
[10] C. Didraga, A. Pugžlys, P.R. Hania, H. von Berlepsch, K. Duppen, J. Knoester, J. Phys. Chem. B 108 (2004) 14976.
[11] F.C. Spano, S. Mukamel, J. Chem. Phys. 91 (1989) 683.
[12] D.G. Lidzey, A.I. Tartakovskii, M. Emam-Ismail, M.S. Skolnick, S. Walker, Synthetic Met. 127 (2002) 151.
[13] A. Chowdhury, S. Wachsmann-Hogiu, P.R. Bangal, I. Raheem, L.A. Peteanu, J. Phys. Chem. B 105 (2001) 12196.
[14] S. Dähne, Bunsen-Magazin 4 (2002) 81.
[15] J. Franck, E. Teller, J. Chem. Phys. 6 (1938) 861.
[16] J. Frenkel, Phys. Rev. 37 (1931) 17.
[17] Z. Zhao, F.C. Spano, J. Chem. Phys. 122 (2005) 114701.
[18] E.W. Knapp, P.O.J. Scherer, S.F. Fischer, Chem. Phys. Lett. 111 (1984) 481.
[19] P.O.J. Scherer, S.F. Fischer, Chem. Phys. 86 (1984) 269.
[20] F.C. Spano, S. Siddiqui, Chem. Phys. Lett. 314 (1999) 481.
[21] A.V. Malyshev, V.A. Malyshev, F. Domínguez-Adame, Phys. Rev. B 70 (2004) 172202.
[22] A. Eisfeld, J.S. Briggs, Chem. Phys. 281 (2002) 61.
[23] J.S. Briggs, A. Herzenberg, J. Phys. B 3 (1970) 1663.
[24] J.S. Briggs, A. Herzenberg, Mol. Phys. 21 (1971) 865.
[25] W.T. Simpson, D.L. Peterson, J. Chem. Phys. 26 (1957) 588.
[26] G. Scheibe, Kolloid Z. 82 (1938) 1.
[27] S. Al-khouri, Ph.D. Thesis, Universität Duisburg-Essen, 2003.
[28] J.S. Briggs, Z. Phys. Chem. 75 (1971) 214.
[29] B. Neumann, J. Phys. Chem. B 105 (2001) 8268.
[30] M. Lindrum, I.Y. Chan, J. Chem. Phys. 104 (1996) 5359.
[31] C. Spitz, S. Dähne, Ber. Bunsen. Phys. Chem. 102 (1998) 738.
[32] C. Spitz, J. Knoester, A. Ouart, S. Daehne, Chem. Phys. 275 (2002) 271.